Frustration-driven spin freezing in the $S=\frac{1}{2}$ fcc perovskite Sr_2MgReO_6

C. R. Wiebe,[1,4] J. E. Greedan,[2,*] P. P. Kyriakou,[1] G. M. Luke,[1] J. S. Gardner,[3] A. Fukaya,[4] I. M. Gat-Malureanu,[4] P. L. Russo,[4] A. T. Savici,[4] and Y. J. Uemura[4]

[1]*Department of Physics and Astronomy, McMaster University, Hamilton, Ontario L8S 4M1, Canada*

[2]*Department of Chemistry, McMaster University, Hamilton, Ontario L8S 4M1, Canada*

[3]*NIST Center for Neutron Research, NIST, Gaithersburg, Maryland 20899-8562, USA and Physics Department, Brookhaven National Laboratory, Upton, New York 11973-5000, USA*

[4]*Department of Physics, Columbia University, New York, New York 10027, USA*

(Received 18 March 2003; revised manuscript received 21 July 2003; published 7 October 2003)

The ordered perovskite Sr_2MgReO_6 of tetragonal symmetry [$I4/m$, $a=5.5670(1)$ Å, $c=7.9318(2)$ Å at $T=295$ K] has been synthesized and characterized by x-ray and neutron diffraction, thermal gravimetric analysis dc susceptibility, heat capacity, and muon spin relaxation (μSR) experiments. The B site cations Re^{6+} and Mg^{2+} appear to be ordered due the large difference in formal charge. The Re^{6+} magnetic ions form a distorted fcc lattice of $S=\frac{1}{2}$ spins providing a frustrated topology of edge-shared tetrahedra. The material exhibits a weak magnetic glassiness shown by a cusp at ~50 K in the dc susceptibility, a weak but broad heat capacity anomaly, and a low-temperature μSR line shape characteristic of a spin-glass state. A broad and strongly field- dependent maximum in the dc susceptibility suggests that magnetic correlations persist to ~175 K, accompanied by a divergence in the field-cooled and zero-field-cooled susceptibility. The anisotropic nature of the superexchange pathways due to the tetragonal distortion is thought to disrupt the ideal frustrated environment and lead to weaker glassiness than Sr_2CaReO_6, which has $T_G \sim 14$ K, and a large specific heat anomaly. In contrast, Sr_2MgReO_6 has a small anomaly, and only about 3% of the entropy is released at $T_G \sim 50$ K, which is comparable to other unconventional spin glasses such as the jarosite $(H_3O)Fe_3(SO_4)_2(OH)_6$(~6%). $T_G \sim 50$ K is unusually high for this class of materials.

DOI: 10.1103/PhysRevB.68.134410 PACS number(s): 75.50.Lk, 74.25.Ha, 61.12.−q, 76.75.+i

I. INTRODUCTION

Some of the most fascinating phenomena in condensed matter physics arise from competing interactions.[1] Anderson's prediction of the unusual and interesting physics that would arise out of these systems has been realized experimentally in a wide variety of materials,[2] from high-T_C superconductors[3] to molecular crystals[4] to geometrically frustrated antiferromagnets.[5] In the latter case, the inability of the sublattice to magnetically order often leads to exotic ground states. In particular, the study of $S=\frac{1}{2}$ species on frustrated lattices has been the target of current research with the promise of a ''spin-liquid'' state that is thought to arise in the quantum limit.[6,7] The spin liquid, a dynamic state that is comprised of rapidly fluctuating spin singlets, was inspired by Pauling's resonating valence bond model[8] and later applied by Anderson to spin frustration. In spite of considerable effort to search for such systems, to date very few ideal spin liquids have been discovered.

The current trend in the search for this elusive ground state is centered on low-dimensional systems. Evidence for liquidlike behavior has been noted for two-dimensional (2D) layered systems such as $SrCr_{9p}Ga_{12-p}O_{19}$ (SCGO) (Ref. 9) and $Ba_2Sn_2Ga_3ZnCr_7O_{22}$ (Ref. 10), but very few three-dimensional spin liquids have been well characterized. Most three-dimensional systems in fact show spin glassiness, such as the pyrochlore $Y_2Mo_2O_7$, in which the moments ''freeze out'' and only short-range order is observed.[11] There are a few exceptions, such as $Tb_2Ti_2O_7$, which enters a ''cooperative paramagnetic state'' at low temperatures,[12] but overall the literature is lacking clear examples of three-dimensional liquidlike materials.

The perovskites have largely been overlooked as structures that can be used as a framework for frustrated magnetic sublattices. B-site ordered double perovskites of the form $A_2BB'O_6$ have been demonstrated to be extremely stable to substitution of various ions upon the B and B' sites, each of which form independent fcc sublattices.[13] This provides the opportunity to study frustration effects, as the fcc lattice forms a network of edge-shared tetrahedra. Traditionally, most fcc materials enter long-range ordered ground states, and it is indeed this lattice that was first studied as the canonical example of an ordered antiferromagnet in early neutron scattering measurements on binary oxides such as MnO.[14] However, in the binary oxides, near-neighbor and further-neighbor interactions compete and eventually favor the formation of an ordered ground state. This problem is somewhat alleviated in the double perovskites, as the lattice is much more dilute with nearest neighbors separated by ~5 Å and a correspondingly diminished role for further neighbors. The choice of a Re cation on the B sites is essential to provide good overlap between the sites relying on the larger spatial extent of the $5d$ orbitals. Incidentally, the magnetism of the $5d$ electrons in the Re cation has recently attracted considerable attention. For example, the metal-insulator transition in Sr_2FeReO_6 (Ref. 15) and the superconducting pyrochlore $Cd_2Re_2O_7$ (Ref. 16) have been objects of fruitful study as of late.

This paper details an in-depth study of the ordered perovskite, Sr_2MgReO_6, which presents the combination of quantum magnetism with a topologically frustrated sublattice. The related material Sr_2CaReO_6, which is a distorted perovskite of monoclinic symmetry, shows spin glass behavior with $T_G \sim 14$ K.[17] Several conventional spin-glass-like features were seen, such as a cusp in the dc susceptibility, the lack of long-range magnetic order, magnetic hysteresis, and spin freezing noted by muon spin relaxation (μSR) experiments. However, a few unusual properties were discovered as well. The appearance of a low-temperature field-independent specific heat anomaly with a T^3 dependence in particular suggested that a spin singlet ground state may be present that is stabilized by strong 3D spin fluctuations. The magnetic character of Sr_2MgReO_6, which has tetragonal rather than monoclinic symmetry, is markedly different from the Ca material, but these new properties can be understood by investigating the differences in the crystal structure and the magnetic exchange paths. The properties of these two materials will be compared to $S=1$ analogs (Sr_2NiMO_6, $M=$ W or Te) to emphasize the role of quantum effects in this low-spin system.

II. EXPERIMENTAL PROCEDURES

The original structural report on this material was by Ferretti, Rogers, and Goodenough,[18] who made samples by firing stoichiometric amounts of $SrCl_2$, $KReO_4$, Re, SrO, and MgO in sealed evacuated tubes followed by washing well with water to remove KCl:

$$3\,SrCl_2 + 6\,KReO_4 + Re + 11\,SrO + 7\,MgO \rightarrow 6\,KCl + 7\,Sr_2MgReO_6. \quad (1)$$

Attempts to synthesize the sample by this method were unsuccessful.

Powder samples of Sr_2MgReO_6 were synthesized by combining stoichiometric amounts of SrO (99.9%, Fisher), MgO (99.95%, Alfa-Aesar), and ReO_3 (99.9%, Rhenium Alloys, Inc.), and then firing under vacuum for 60 h in platinum crucibles at 900 °C:

$$2\,SrO + MgO + ReO_3 \rightarrow Sr_2MgReO_6. \quad (2)$$

The starting materials SrO and MgO were prefired under vacuum for 12 h at 400 °C in separate ceramic containers to remove any absorbed water or surface impurities.

The phase purity of the final product was tested using a focusing Guinier-Hägg camera with copper $K\alpha_1$ radiation and Si powder as an internal standard. After several firings, no impurities were detected using this technique. Thermogravimetric analysis was used to determine the oxygen stoichiometry by reducing the sample in a hydrogen atmosphere at 900 °C.

A Bruker D8 diffractometer using Cu $K\alpha_1$ radiation was used to obtain high-resolution x-ray diffraction patterns. Initial analysis of powder x-ray diffraction data using the search routine[19] DICVOL indicated that the sample was single phase. The software package[20] FULLPROF was used to refine the room temperature crystal structure.

This material was also examined using neutron diffraction at the C2 beamline of the National Research Council's Neutron Program for Materials Research in Chalk River, Canada. Using data collected with neutron wavelengths of $\lambda = 1.3285(3)$ Å and 1.32812(4) Å, the crystal structure was refined at 6 K and room temperature using FULLPROF.[20] Neutron diffraction measurements showed that there was indeed a small MgO impurity (0.6%) in the sample not detected with x rays. Since no other impurities were found, this was assumed to be due to either a small weighing error or an incomplete reaction.

The dc magnetic susceptibility was measured using a Quantum Design MPMS SQUID magnetometer at McMaster University. Field-cooled (FC) and zero-field-cooled (ZFC) scans were made over a temperature range of 2 K to 350 K under various applied magnetic fields. Isothermal magnetization scans were also obtained at 5 K and 250 K over the field range ± 0.4 T.

An Oxford Instruments calorimeter probe in the Oxford Instruments MAGLAB apparatus was used to measure the heat capacity of this sample. A pellet of mass 12.19 mg was attached to the probe using a measured portion of Wakefield grease (for which a correction was made using software provided by Oxford Instruments). The measurements were made between 3 K and 70 K using the relaxation method. Measurements were also completed on the lattice standard Sr_2MgWO_6 over the same temperature range to estimate the lattice contribution to the specific heat. The measurements were carried out in a similar fashion with a pellet of mass 9.80 mg.

μSR experiments were completed at the M15 beamline at TRIUMF in Vancouver, Canada. The measurements were made over a temperature range of 2.5 K to 130 K in a small applied longitudinal field of 65 G. A series of longitudinal field measurements up to 2065 G were made at 5 K.

III. RESULTS AND DISCUSSION

A. Crystal structure

Ferretti *et al.* reported the structure of Sr_2MgReO_6 to be tetragonal, but no cell constants or space groups were given.[18] Indexing of the Bragg peaks determined the space group to be $I4/m$. Our room temperature lattice parameters, as determined from Rietveld refinement of x-ray diffraction data, were $a = 5.5670(1)$ Å and $c = 7.9318(2)$ Å.

Structure refinements were done at 6 K and 295 K using neutron diffraction data. The results are listed in Table I, with the full diffraction pattern displayed in Fig. 1. The small MgO impurity is noted as the second set of tick marks in the diffraction pattern. The calculated weight percentage of MgO was found to be 0.6% by Rietveld refinement.

As these samples were prepared under vacuum, there was some concern about the oxygen stoichiometry. A defect structure would be difficult to detect by x-ray diffraction or with the limited Q space surveyed by our neutron diffraction experiments (which were primarily used to detect magnetic ordering and disorder on the cation sites). Several thermal gravimetric analysis (TGA) experiments were conducted up

TABLE I. Lattice parameters for Sr_2MgReO_6 at 6 K (neutron data) and 295 K (neutron and x-ray data) as determined by powder diffraction. The material used as a model for the lattice contribution to the heat capacity, Sr_2MgWO_6, is referenced as well for comparison (x-ray data).

	Neutron data		X-ray data	
	Sr_2MgReO_6, 6 K (Å)	Sr_2MgReO_6, 295 K (Å)	Sr_2MgReO_6, 295 K (Å)	Sr_2MgWO_6, 295 K (Å)
a	5.5350(6)	5.5647(3)	5.5670(1)	5.5816(1)
c	7.9724(9)	7.9323(5)	7.9318(2)	7.9420(1)

to 900 °C to reduce Sr_2MgReO_6 to SrO, MgO, and Re metal under flowing hydrogen to measure the weight loss, and thus the oxygen stoichiometry:

$$Sr_2MgReO_6 + 3H_2 \rightarrow 2SrO + MgO + Re + 3H_2O. \quad (3)$$

The final solid state products were confirmed by x-ray powder diffraction using a Guinier-Hägg camera to ensure that the reaction was complete. The theoretical weight loss was 9.96%. The average of several of these reactions was 9.75(10)% weight loss. Thus, the sample is nearly stoichiometric with respect to oxygen. The slight deficiency may be due to the small amount of excess MgO remaining in the sample, which would lower the expected weight loss.

The crystal structure of Sr_2MgReO_6 is shown in Fig. 2. Several detailed refinements of the structure were attempted using models of disorder upon the *B* and *B′* sites (see Table II). The site occupancies were refined to within 1% of full occupation by Mg and Re, respectively, in both the neutron and x-ray work. The electrostatic repulsion between the Re^{6+} and Mg^{2+} species is thought to be a significant ordering mechanism. The significant difference in ionic radii (0.86 and 0.69 Å for Mg and Re with VI coordination)[21] will also aid the cation ordering. The relatively large size of the Sr^{2+} cation excluded the possibility of disorder on this site as well (which is 1.18 Å for VI coordination). The occupation of the oxygen sites were allowed to vary in the final refinements, but they did not change appreciatively from full occupation.

The ideal material to study the magnetic properties of fcc magnetic sublattices would be the cubic case, as all of the bond angles and exchange paths would be identical for the interconnected tetrahedra. In the case of Sr_2MgReO_6 the structure is tetragonal, and the exchange paths are anisotropic. The Re-O-Mg bond angles are fixed to 180 ° by symmetry along the *c* direction, but they are distorted in the *ab* plane to 165.57(19)°, as shown in Fig. 2(b) and Table III (at 6 K). The tetragonal distortion also results in slightly different Re-Re bond distances, but these vary by less than 1% (see Fig. 3). The significant differences in bond angles, and thus $5d$ orbital overlap, are believed to play a much more important role.

It is worth noting that this distortion away from cubic symmetry has been observed for the Ca analog Sr_2CaReO_6. It is believed that the relatively small size of the *A* cation

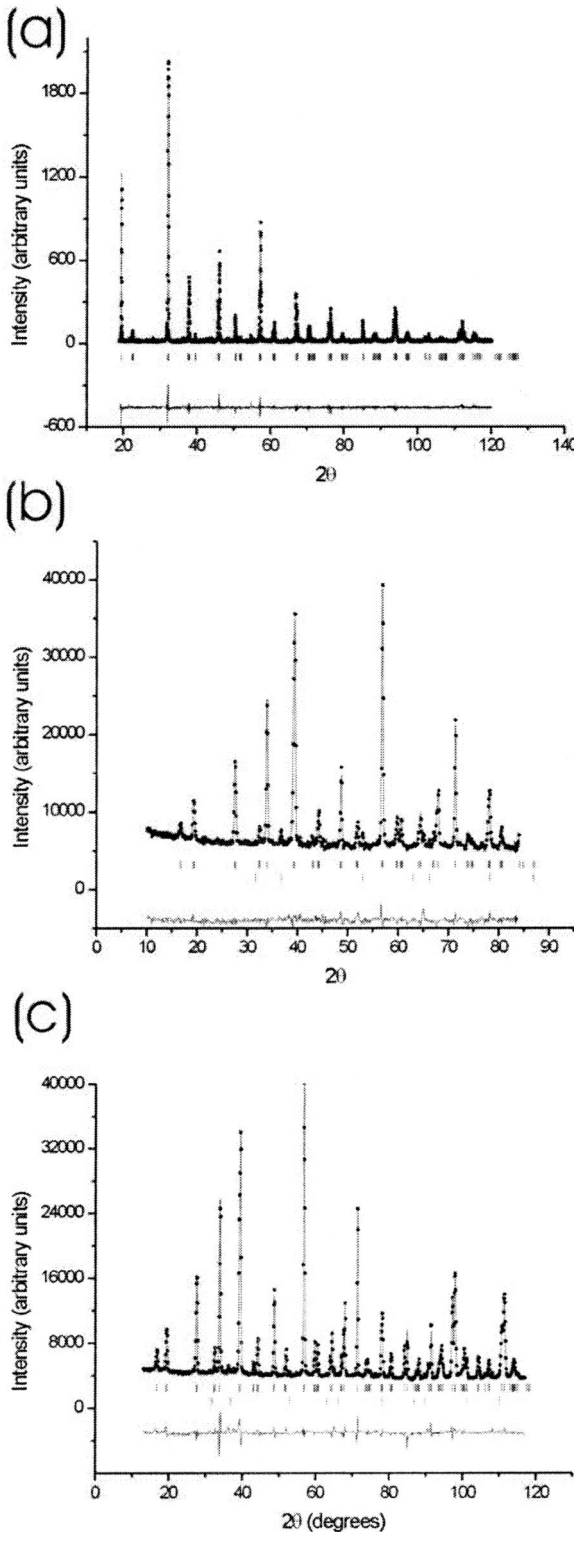

FIG. 1. (a) Powder x-ray diffraction refinements of Sr_2MgReO_6 at $T=298$ K with Cu $K\alpha_1$ radiation. ($R_p=12.2$, $R_{wp}=17.4$). (b) Powder neutron diffraction refinement of Sr_2MgReO_6 at $T=6$ K with $\lambda=1.3285(3)$ Å. ($R_p=2.86$, $R_{wp}=4.06$). The second set of tick marks is for a small MgO impurity. (c) Powder neutron diffraction refinement of Sr_2MgReO_6 at $T=295$ K with $\lambda=1.32812(4)$ Å. ($R_p=3.17$, $R_{wp}=4.03$.) The second set of tick marks is for a small MgO impurity.

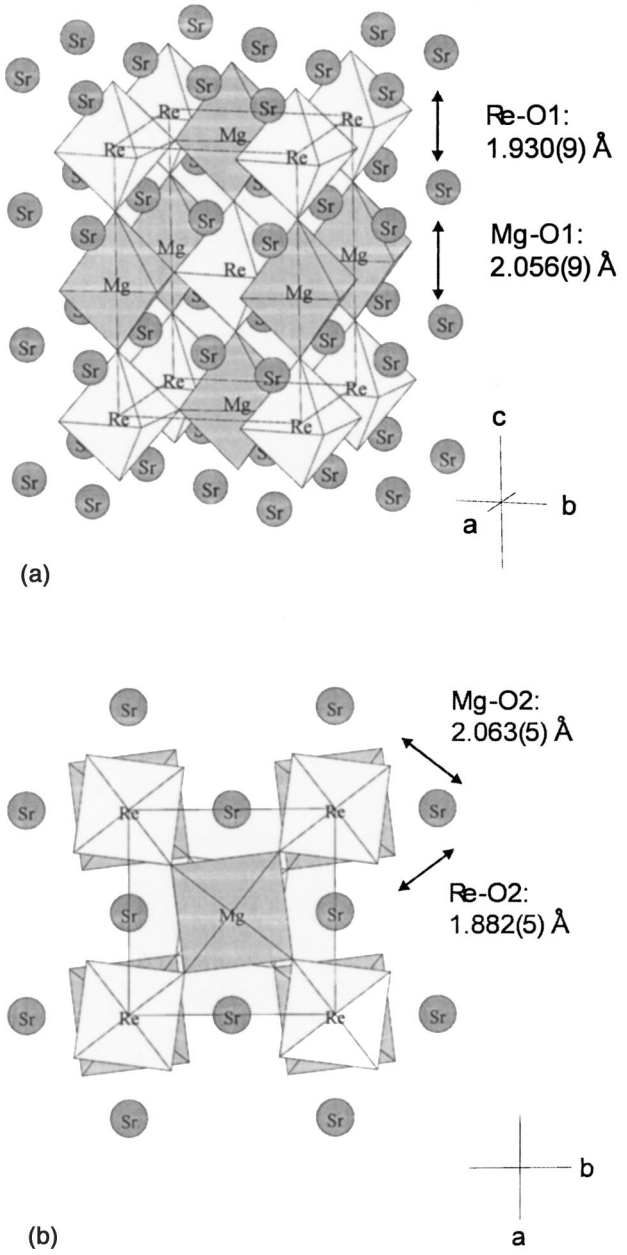

FIG. 2. (a) The crystal structure of Sr_2MgReO_6 as viewed oblique to the *ac* plane. (b) The crystal structure of Sr_2MgReO_6 as viewed normal to the *ab* plane.

facilitates this distortion to a monoclinic structure. Indeed, Ba_2CaReO_6, with its larger Ba^{2+} cation (1.61 Å compared to Ca^{2+} of 1.44 Å) is cubic.

The structural difference between Sr_2CaReO_6 and Sr_2MgReO_6 is due to the relative sizes of the *B* site cations. In the monoclinic case (Sr_2CaReO_6), the difference between Ca^{2+} and Re^{6+} is large (1.00 Å and 0.69 Å respectively), which leads to a distortion of their respective octahedra to fill space. In the case of Mg^{2+} and Re^{6+}, the sizes are more similar (0.86 Å for Mg^{2+}), and thus the distortion is only a slight twisting in the *ab* plane.

Due to the centrosymmetric crystal structure presented here, the previously reported room-temperature ferroelectric phase[22] and the associated Jahn-Teller distortions are difficult to imagine. Neutron data suggest that there is a slight elongation of the Re-O bonds in the *c* direction, but this small variation [1.930(9) Å for Re-O1 and 1.882(5) Å for Re-O2 at 6 K] makes it hard to justify Re^{6+} as a true Jahn-Teller active ion in this material. However, it should be noted that Re-O bond distances are significantly more distorted than the Sr_2CaReO_6Re octahedra [1.907(4) Å for Re-O1, 1.921(5) Å for Re-O2, and 1.904(4) Å for Re-O3]. There is no such distortion for the Mg-O distances, which change very little from 6 K to 295 K. In general, Jahn-Teller effects are more subtle for t_{2g}^1 configurations than for e_g^1, and it is difficult to confirm whether or not this is a real effect in this material based upon this study alone. The literature of Jahn-Teller effects in Re^{6+} species is very sparse.

TABLE II. Refined lattice positions and temperature factors for Sr_2MgReO_6 [$\lambda = 1.3285(3)$ Å] at 6 K [and 295 K, $\lambda = 1.32812(4)$ Å in parentheses].

	x	*y*	*z*	*B* (Å^2)	Site
Sr	0	0.5	0.25	0.456(10) (0.62(3))	4*d*
Mg	0	0	0.5	0.10(1) (0.18(2))	2*b*
Re	0	0	0	0.07(1) (0.13(1))	2*a*
O1	0	0	0.242(1) (0.2426(9))	0.493(8) (0.72(7))	4*e*
O2	0.2700(9) (0.2657(7))	0.2066(7) (0.2140(5))	0	0.565(10) (0.69(4))	8*h*

B. Magnetic susceptibility experiments and neutron diffraction

Although Sr_2MgReO_6 has been known for some time, there are no detailed reports of the magnetic properties. Ferretti *et al.* found that Sr_2MgReO_6 had a room-temperature resistivity that is in the semiconductor to insulator regime of at least 10^5 Ω cm.[18] The conclusion was that the *d* electrons

TABLE III. Bond distances and angles for Sr_2MgReO_6 at $T = 6$ and $T = 295$ K as determined by powder neutron diffraction. There are no appreciable changes due to the phase transition at $T_G \sim 50$ K. The average distances for the Re-O and Mg-O bonds are in good agreement with the values listed by Shannon (Ref. 21) for Re^{6+}-O (1.90 Å) and Mg^{2+}-O (2.07 Å).

	6 K	295 K
Re-O1 (Å)	1.930(9)	1.926(8)
Re-O2 (Å)	1.882(5)	1.901(4)
Mg-O1 (Å)	2.056(9)	2.040(8)
Mg-O2 (Å)	2.063(5)	2.055(4)
Re-Re (Å)	5.5830(6)	5.5647(3)
	5.5864(4)	5.5869(2)
Re-O2-Mg (deg)	165.57(19)	168.17(16)
Re-O1-Mg (deg)	180	180

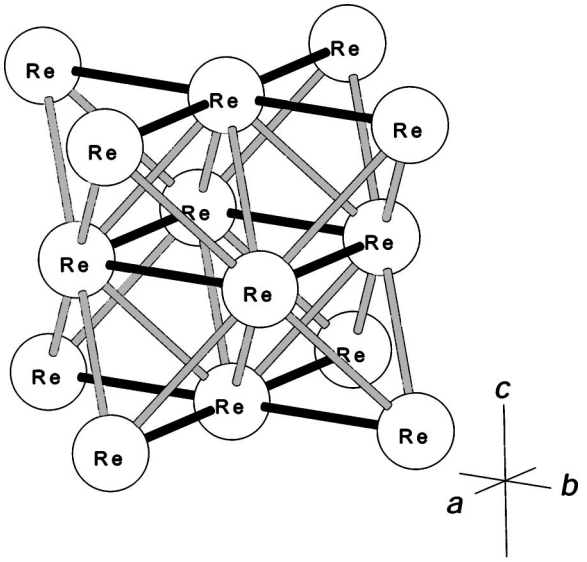

FIG. 3. The fcc ordered sublattice of Sr_2MgReO_6. The two different Re-Re bond distances are marked as 5.5350(6) Å (black bonds) and 5.5864(4) Å (grey bonds).

were localized on the rhenium sites rather than forming a band structure such as that in the parent compound ReO_3. Other than this brief entry, there are no other published results on this material.

Even with full localization on the Re sites, the magnetic susceptibility was expected to be weak, since the electronic configuration is $5d^1$ and the magnetic ions are quite dilute. It was found that a Curie-Weiss regime did not develop in this sample until temperatures of at least 450 K. The resulting fit in Fig. 4 was made to the following relationship:

$$\chi = C/(T-\theta)+\alpha, \tag{4}$$

where $\mu_{\text{eff}}=(8C)^{1/2}$, θ is the Weiss temperature, and α is a temperature-independent paramagnetic term (TIP). A correction for the diamagnetism of the sample was made before the Curie-Weiss fits were completed. In the range of 450 K–600 K and under a field of 1 T, the Weiss temperature was found to be $\theta=-426(58)$ K and $\mu_{\text{eff}}=1.72(9)\mu_B$. A very small TIP of $\alpha=0.00009(2)$ EMU/mol was found. These values are similar to those for Sr_2CaReO_6 [where $\mu_{\text{eff}}=1.659(6)\mu_B$ and $\theta=-443(6)$ K], reinforcing the similarities of these two materials. With similar exchange paths and Re-Re distances, it is no surprise that such a comparison can be made. The large and negative Weiss temperature indicates the presence of strong antiferromagnetic interactions, and the value for the effective moment agrees well with the ideal spin-only $S=\frac{1}{2}$ case of $1.73\mu_B$.

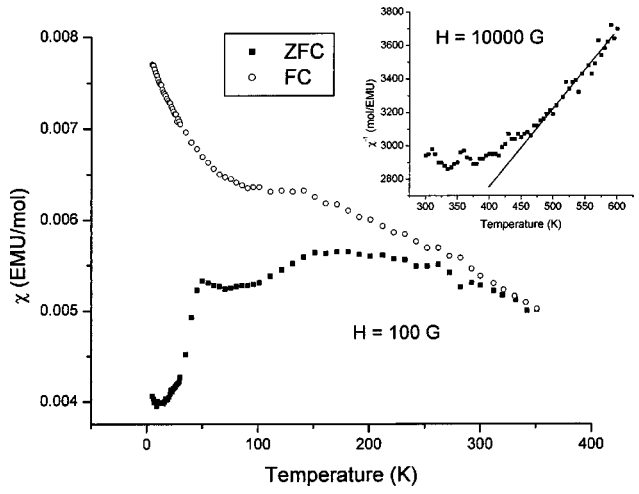

FIG. 4. dc magnetization measurements as a function of temperature at $H=100$ G. Note the cusp at ~50 K and broad feature at ~175 K. The inset shows the Curie-Weiss fit to the high-temperature data, which as taken in a field of $H=10000$ G.

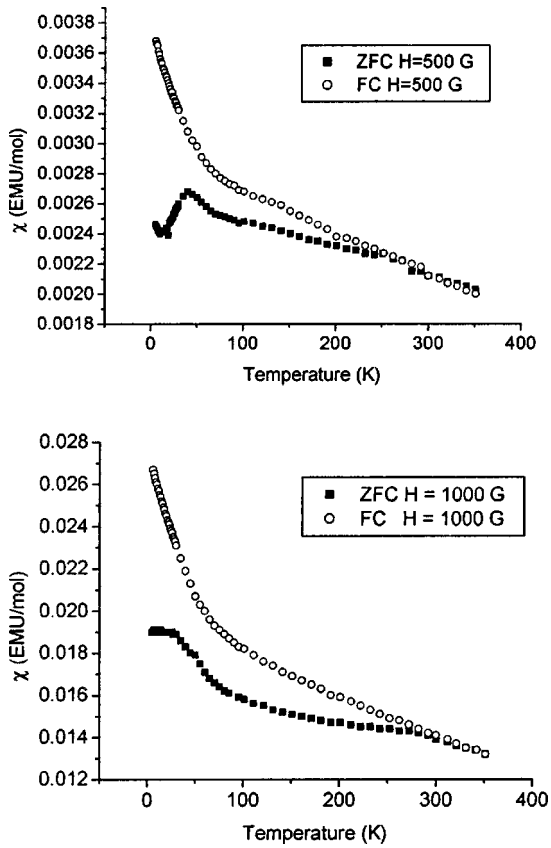

FIG. 5. dc magnetic susceptibility runs for $H=500$ G and 1000 G. Note the disappearance of the 50 K feature and the loss of the broad maximum at 175 K as the field increases.

The lack of a Curie-Weiss regime until very high temperatures is somewhat unusual, as most geometrically frustrated materials tend to exhibit this behavior to temperatures much lower than θ. The reason for this discrepancy is that there is a weak feature in the susceptibility that appears at ~175 K (see Fig. 4). This broad maximum is only present at low fields, and believed to have a long tail that persists to high temperatures. In fields greater than ~500 G, the feature is lost in the background but a clear FC/ZFC divergence is seen that persists to ~250 K (see Fig. 5).

The other notable feature in the data is the cusp and strong FC/ZFC divergence at ~50 K. This is most prominent in the 100 G data set, but evidence is clearly seen in higher fields as a broad maximum. Neutron diffraction measure-

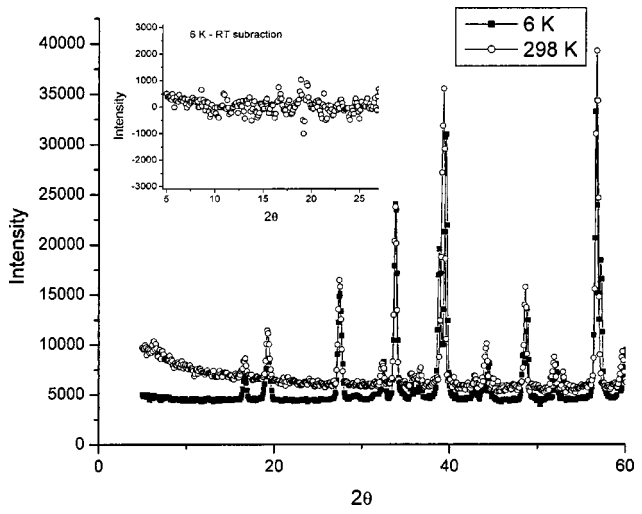

FIG. 6. Powder neutron diffraction scans taken at 6 K and 295 K. The high-temperature run has a slightly higher background due to air scattering. The inset shows a subtraction of the room-temperature data (corrected for air scattering) from the 6 K data.

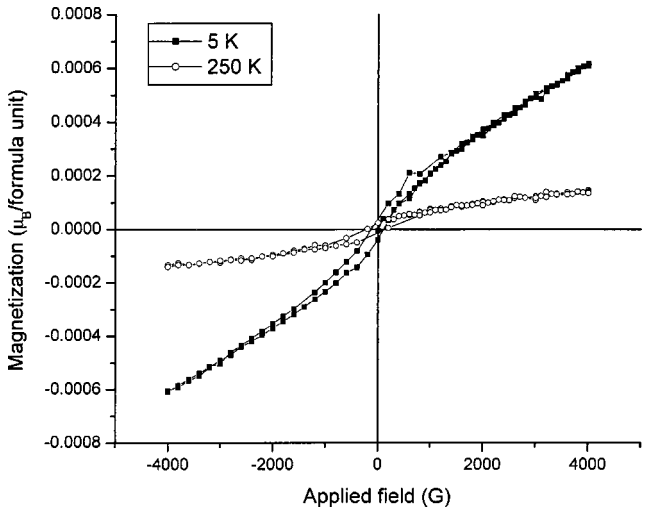

FIG. 7. Magnetic hysteresis runs at 5 K and 250 K for Sr_2MgReO_6. A small temperature-dependent hysteresis is observed.

ments were made at 6 K and room temperature using short-wavelength neutrons [$\lambda = 1.3285(3)$ Å] to search for magnetic ordering. There were no magnetic Bragg peaks found upon inspecting the 298 K and 6 K data (see Fig. 6). There is a small anomaly at $2\theta \sim 29°$, but this is due to a detector problem. Upon changing the wavelength, this feature does not move in 2θ, demonstrating that it is an artifact of the instrument. However, a caveat is needed here when precluding the existence of magnetic ordering: the Re^{6+} ($S = \frac{1}{2}$) moment size is very small, and the magnetic ions comprise only 10% of the atoms in the lattice. Even if the transition at ~50 K in the magnetic susceptibility were a signature of a long-range ordered ground state, it might be difficult to discern such a feature using neutron scattering at a medium flux reactor (and with a small sample size of ~4 g). Simulations show that for an ordered Re^{6+} moment of $1.00\mu_B$, the resulting magnetic Bragg peaks from a type-I structure typical of fcc lattices would be on the order of ~1% of the strong structural peaks.[17] While these would be observable, any reduction in the ordered moment (common for a frustrated system) or a more complex magnetic structure would render these reflections indistinguishable from the background. As a result, other methods were needed to elucidate the nature of the magnetic ground state.

One can compare this system to the $S = 1$ analog Sr_2NiWO_6, which has a Weiss constant of -175 K.[23] As described in the work on Sr_2CaReO_6, the difference in these values can be understood in terms of the more extended nature of the $5d$ orbitals as compared to the $3d$. According to mean-field theory, and neglecting further-neighbor interactions, the nearest-neighbor exchange constants for an fcc lattice can be calculated by

$$J_{\mathrm{NN}}/k = \frac{\theta_c}{12(2/3)S(S+1)}. \tag{5}$$

Thus, the ratio of J_{NN}/k for Sr_2MgReO_6 relative to Sr_2NiWO_6 is 6:1, which is indicative of the larger spatial extent of the $5d$ orbitals. This is comparable to the 5:1 ratio found in Sr_2CaReO_6.[17]

The transition at 50 K in Sr_2MgReO_6 is remarkably similar to what is seen in Sr_2NiWO_6, which has a broad maximum in χ at a Néel temperature of $T_N = 54$ K. However, there is no FC/ZFC divergence in the Ni analog. This history dependence is a common property of frustrated systems that show glassy behavior, such as the pyrochlore $Y_2Mo_2O_7$. However, the broad maximum seen at ~175 K in Sr_2MgReO_6 and the FC/ZFC divergence at 250 K both suggest that magnetic correlations set in at temperatures much higher than T_G. This phenomenon is also present in Sr_2CaReO_6, which has a glassy transition at ~14 K, but a FC/ZFC divergence at ~23 K. In the case of Sr_2MgReO_6, the strong anisotropy of the Re-O-Mg-O-Re exchange paths, which involve 180° linkages along c but 165.57(19)° Re-O-Mg pathways in the ab plane, might bring a one-dimensional character to the magnetism, which could manifest itself as a broad feature in the susceptibility. Sr_2CaReO_6 is virtually isotropic, with respect to exchange pathways, as the Re-O-Ca-O-Re bond angles have a mean of ~153(2)°. In this material there is no indication of low-dimensional magnetism.

Hysteresis loops were also measured at 5 K and 250 K (see Fig. 7). A very small hysteresis was noted in both data sets. This is further evidence for spin clustering, recalling that the FC/ZFC divergence occurs at $T > 250$ K. There could also be a small ferromagnetic impurity that was not detected by either neutron or x-ray diffraction.

C. μSR measurements

The technique of μSR is well established as a standard tool in the study of magnetic materials.[24] The remarkable sensitivity of the muon to local fields and fluctuations thereof, over a wide range of time scales, places μSR as one of the best methods to measure both the statics and dynamics of quantum magnetism.[25]

Measurements were taken in a small applied longitudinal field of 65 G at the M15 beamline at TRIUMF in the tem-

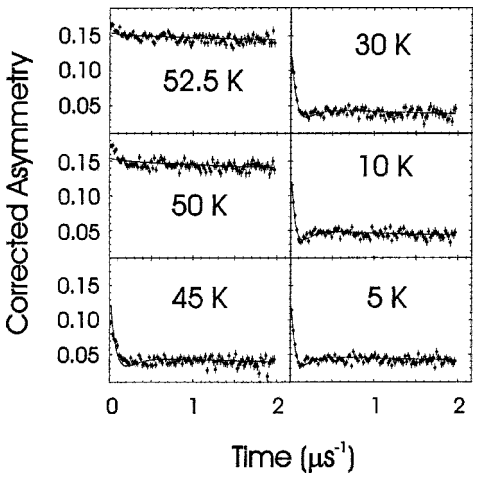

FIG. 8. Longitudinal field μSR data as a function of temperature. The fits are to Eq. (6) as described in the text. Note the dramatic change in line shape below $T_G \sim 50$ K.

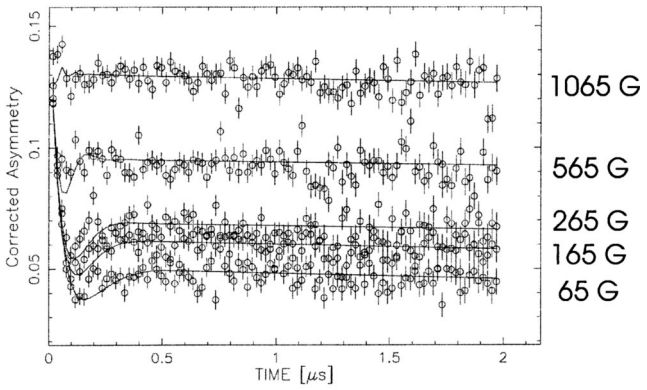

FIG. 9. Longitudinal field μSR runs as a function of field at $T = 5$ K. The fits to the data are Lorentzian functions as described in the text. This shows that the signal is successfully decoupled in moderate fields.

perature range 2 K$<T<$52.5 K; typical spectra are shown in Fig. 8. The small field served to decouple any relaxation from nuclear dipole moments (of typical strength of a few gauss) but was weak enough not to affect the relaxation of electronic origin.

The spectra at all temperatures were well described by the Lorentzian spin-glass relaxation function,[26]

$$G(t)=\frac{1}{3}\{\exp[-(4\alpha_d^2 t/\nu)^{1/2}]\} + \frac{2}{3}\left[1-\frac{\alpha_s^2 t^2}{(4\alpha_d^2 t/\nu+\alpha_s^2 t^2)^{1/2}}\right] \times \exp[-(4\alpha_d^2 t/\nu+\alpha_s^2 t^2)^{1/2}], \quad (6)$$

where α_s and α_d are the static and dynamic portions of the moment respectively, and ν is the fluctuation rate. The development of a static portion of the moment is apparent from the two-component form of the relaxation seen below about 50 K (see Fig. 8). The order parameter Q is

$$Q=\left(\frac{\alpha_s}{\alpha}\right)^2, \quad \alpha^2=\alpha_s^2+\alpha_d^2. \quad (7)$$

As $\alpha_d \rightarrow 0$, this function reduces to a Lorentzian Kubo-Toyabe (KT) function:

$$G(t)=\tfrac{1}{3}+\tfrac{2}{3}[1-\alpha_s t]\exp(-\alpha_s t), \quad (8)$$

which is appropriate for a dilute source of randomly aligned magnetic moments. The Lorentzian KT function gave an essentially identical fit to the low-temperature data.

It is worth indicating at this point that several longitudinal field scans were made to confirm the origin of these spectra. Field scans up to 1065 G successfully decoupled the signal, as shown in Fig. 9. This directly shows that the response is from the frozen moments within the sample. The fits to the data are Lorentzians, which, as suggested above, are identical to the spin glass function [Eq. (6)] in the low-temperature limit, and easier to handle numerically with a large applied longitudinal field.

The two-component nature of the low-temperature spectra is readily apparent from the data and is typical of spin-glass behavior. The appearance of a second component at $T_G \sim 50$ K agrees well with the dc susceptibility measurements that indicate a glasslike state at this temperature. This feature grows over a temperature range of about a decade, in sharp contrast to the situation in Sr_2CaReO_6, in which the line shape changes dramatically over a few kelvins. Nonetheless, the extraction of an order parameter, Q, from the spin glass function can be made to illustrate the nearly first-order nature of the transition.

As Fig. 10 shows, the freezing of the moments is very abrupt. Power law fits to the order parameter were made, but no sensible exponents could be found. Figure 10 also displays the fluctuation rate as a function of temperature, which is correlated with the appearance of the static order parameter below T_G. Above T_G, the spins are paramagnetic, leading to a nearly temperature-independent fast fluctuating rate. It is quite likely that these measurements are very near or beyond the detection limits of this technique. However, at the transition itself, there is a rapid drop in the fluctuation rate. From 50 K to 10 K, there is a decrease of over six orders of magnitude. This is a clear signal for spin freezing. Below 10 K, the fluctuation rate is very small, or virtually undetectable in this limit, which is evident in the flat background of the lineshape, which indicates very slow fluctuations. Such behavior is what one would expect for a glassy system: a slowing down of moments over a wide range of frequencies[27] ($\sim 10^8$) and a high-temperature paramagnetic regime (hence the temperature-independent response in the extremes). The line drawn in the figure demonstrates the exponential decrease in the fluctuation rate over a wide range of frequencies below T_G.

The abrupt onset of the order parameter may be an artifact of the fitting function chosen to analyze the Sr_2MgReO_6 data. This function is obtained by assuming a single fluctuation time, a Markovian correlation of spin fluctuations, and a

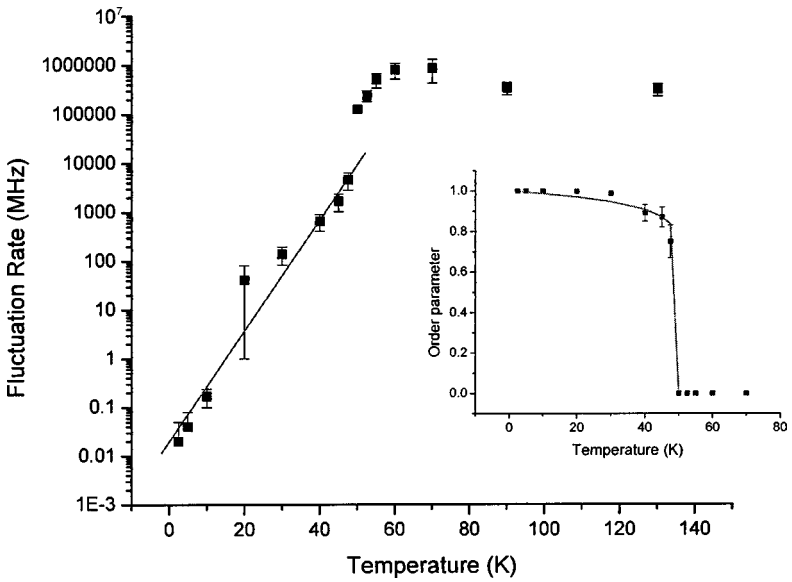

FIG. 10. The fluctuation rate as a function of temperature, indicating moment freezing below T_G. The line drawn is a guide to the eye, demonstrating the exponential nature of the freezing. The inset shows the static order parameter, Q, as a function of temperature. The line is a guide to the eye.

Lorentzian distribution of local fields.[26] In actual spin glasses, these assumptions are often violated (for example, there is usually a distribution of correlation times near T_G, and for dense glasses, a Gaussian distribution of local fields). A modified function that would, in particular, provide better fits to the data near T_G would probably indicate a transition that has more second-order character rather than such a sudden first-order-like change in the order parameter.

In comparison to other spin glasses, such as Sr_2CaReO_6, the data are qualitatively similar. The spin-glass function provides an excellent fit, which is further evidence for spin freezing. However, Sr_2MgReO_6 has a much more pronounced minimum in the spectra. There is also more quantitative evidence in this work that confirms that the material is glassy by showing a dramatic fall of the fluctuation rate below T_G. More measurements are clearly needed in the Sr_2CaReO_6 material for a proper comparison.

In broader terms, the characteristic spectra of Sr_2MgReO_6 are similar to what is seen in other geometrically frustrated spin glasses. $Y_2Mo_2O_7$ has this characteristic at low temperatures, with a pronounced minimum at short time scales and an impressive drop in fluctuation rate below T_G.[28] In contrast though, there are significant dynamics above T_G in $Y_2Mo_2O_7$ that were later identified by neutron scattering to be due to low-energy magnetic excitations. It is difficult to tell if these persistent fluctuations are present in Sr_2MgReO_6, as the fluctuation rate at low temperatures is approaching the limit of what is detectable by μSR. The dynamics are certainly much more suppressed in Sr_2MgReO_6.

No correlation could be found with the high-temperature FC/ZFC divergence present in the susceptibility in Sr_2MgReO_6. If there were short-ranged ordering for example in this sample, this would manifest as a weak precession signal superimposed upon the spectra. Since no such feature is present, we must conclude that, at least, no such ordering occurs over time scales accessible to both neutrons and μSR, which is over nine orders of magnitude. Given this information, one may propose that the broad maximum and FC/ZFC divergence in the susceptibility at high temperatures are due to a ''frustration'' component, as suggested by Limot *et al.* for SCGO.[29] Ga-NMR measurements on this material indicated that magnetic correlations persist up to an intermediate temperature scale of $\sim$50 K, which is very much higher than $T_G \sim 2$ K for SCGO. Evidence for this effect is in a weak maximum in the susceptibility, which has been interpreted as due to strong 2D correlations. Likewise, the effects seen in Sr_2MgReO_6 at $\sim$175 K may be due to the weak magnetism associated with the frustrated 3D fcc lattice, although an analytical term that can describe such a feature is unknown. The absence of these features in the high-temperature magnetic susceptibility of Sr_2CaReO_6 suggests that the anisotropy in Sr_2MgReO_6 may play a role. Indeed, the preferential exchange path along the c axis may induce some one-dimensional character to the magnetism, which manifests itself in the magnetic susceptibility.

D. Heat capacity measurements

Heat capacity measurements on Sr_2MgReO_6 are shown in Fig. 11. As shown in the inset, the low-temperature behavior follows the empirical law

$$C(T) = \gamma T + \beta T^3, \tag{9}$$

where $\gamma = 1.89(24)$ mJ/(K^2 mol) and $\beta = 0.361(2)$ mJ/(K^4 mol). Other magnetic insulators such as Li_4MgReO_6 (Ref. 30) have dramatically increased γ components (by a factor of 37 in this case), which have been interpreted as a signature of spin glassiness, as it implies a highly degenerate ground state. The γ value reported for Sr_2MgReO_6, albeit small, is unusual in a magnetic insulator and it is surprising that such a good fit could be obtained.

The ordered perovskite Sr_2MgWO_6 was prepared as a lattice standard to permit the isolation of the magnetic component of the specific heat. This material was synthesized by combining stoichiometric amounts of $SrCO_3$ (99.999%, Cerac), $MgCO_3$ (99.999%, Cerac), and WO_3 (99.98%, Alfa-Aesar), pressing the mixture into pellets, and firing at

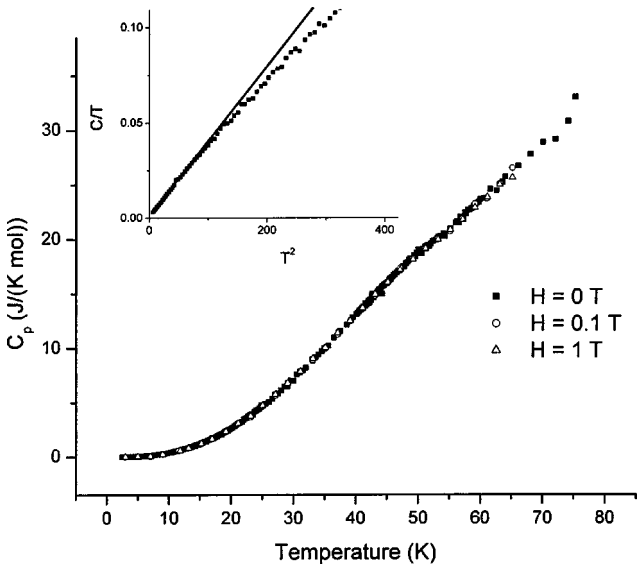

FIG. 11. The heat capacity as a function of temperature and field for Sr_2MgReO_6. The inset is a fit to $C=\gamma T+\beta T^3$, with $\gamma=1.89(24)$ mJ/(K^2 mol) and $\beta=0.361(2)$ mJ/(K^4 mol).

1350 °C in air. The resulting product was confirmed to be single phase and isostructural to Sr_2MgReO_6 by x-ray diffraction (see Table I). This lattice standard was measured using the same method as Sr_2MgReO_6. A sample mass of 9.80 mg was mounted with a small portion of Wakefield grease upon the sample stage. The experiments were performed over the same temperature range as for Sr_2MgWO_6.

The resulting heat capacity is shown in the upper inset to Fig. 12. Remarkably, the data are linear over the temperature range investigated. A scaled lattice portion was calculated and subtracted from the total heat capacity of Sr_2MgReO_6, which is displayed in Fig. 12. It is clear that there is an

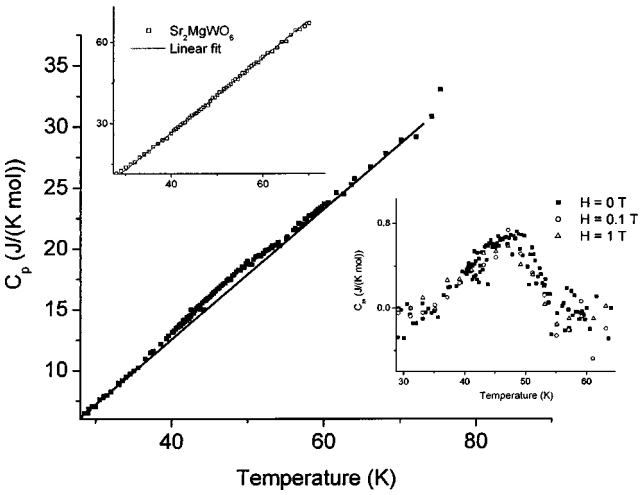

FIG. 12. The scaled lattice component is plotted with the raw data, suggesting that a weak magnetic component is present. The upper inset shows the linear dependence of the lattice standard Sr_2MgWO_6 as a function of temperature. The magnetic specific heat, as determined by a subtraction of the lattice portion, is shown in the lower inset. Note the unchanged feature as a function of field.

anomaly in the vicinity of $T_G\sim 50$ K. However, the feature is very weak and broad, thus ruling out a λ-like anomaly that would be indicative of long-range ordering. The observed broad distribution is suggestive of short-range order. This result is consistent with the neutron diffraction, dc susceptibility, and μSR results, which also point to short-range order and possible spin glassiness below 50 K.

It is interesting to note that there appears to be very little change in the magnetic heat capacity as a function of applied field (Fig. 12). This result was seen in the Ca analog, which had a very broad field-independent specific heat anomaly centered at $T_G\sim 14$ K. The layered kagomé system SCGO also has such a feature, which shows a behavior that is robust to applied fields. Ramirez *et al.*[31] and Sindzingre *et al.*[32] have suggested that such a response is typical of spin-singlet-stabilized ground states, which would be impervious to high magnetic fields due the dynamic nature of the quantum system. If this is true, then this is tantalizing evidence that Sr_2CaReO_6 and Sr_2MgReO_6 have singlet magnetism playing a role at low temperatures. In Sr_2MgReO_6, the entropy removal, as calculated from integrating the magnetic component of the heat capacity from 30 K to 60 K,

$$S=\int_0^T (C_m/T)dT, \tag{10}$$

is extremely small: 0.16738 J/(mol K). This is only about 3% of the ideal amount of $R\ln(2S+1)=5.7628$ J/(mol K). However, it is comparable to what is observed in the jarosite $(H_3O)Fe_3(SO_4)_2(OH)_6$, which has ~6% entropy removal from the magnetic transition.[33] In contrast though, there is no broad anomaly at the transition in this material. In spite of this absence, $(H_3O)Fe_3(SO_4)_2(OH)_6$ is characterized as a spin glass with $T_G\sim 19$ K, and only short-range order at low temperatures. The spin-fluid nature of this material is evident in the T^2 heat capacity dependence at low temperatures. In contrast Sr_2MgReO_6 shows a T^1 dependence at low T which is also field invariant.

On a final note, one can now readily compare the $S=\frac{1}{2}$ systems to their $S=1$ analogs to emphasize the role that quantum spins play upon frustrated lattices. Both $S=1$ materials Sr_2NiWO_6 and Sr_2NiTeO_6 show a long-range ordered state at $T_N=54$ K and 28 K, respectively.[23] In contrast, the $S=\frac{1}{2}$ materials show glassy transitions at $T_G=50$ K and 14 K for Sr_2MgReO_6 and Sr_2CaReO_6, respectively. The similarities between the two sets of transition temperatures reinforce the close structural relationships of the two families of compounds. It is remarkable that the two sets of compounds show similar ordering temperatures yet the $S=\frac{1}{2}$ systems show no long-range magnetic ordering. It is also unusual that the magnetic contribution to the heat capacity shows very little change as a function of applied magnetic field for the $S=\frac{1}{2}$ materials. Canonical spin glasses, such as CuMn, typically show a suppression of the magnetic heat capacity upon application of a field.[34] This is convincing evidence that although these $S=\frac{1}{2}$ systems have been characterized as spin glasses in the absence of disorder, their ground states are poorly understood, and may contain, for example,

mixtures of frozen spins and spin singlets. At present the behavior is clearly very different from the isostructural $S=1$ analogs.

IV. CONCLUSIONS

The *B*-site ordered $S=\frac{1}{2}$ fcc perovskite, Sr_2MgReO_6, has been synthesized and characterized. An apparent transition at ~50 K is seen in the magnetic susceptibility, specific heat, and μSR. The μSR data support a spin-glassy state below 50 K. However, several unusual features, such as a broad maximum in the susceptibility at ~175 K (seen at low applied fields), and the field-independent heat capacity anomaly at T_G are suggestive of liquid behavior. The high temperature (175 K) susceptibility anomaly is not echoed in any other measurement, and is hypothesized to be due to one-dimensional spin correlations induced by the strong 180° superexchange paths along *c*.

ACKNOWLEDGMENTS

The authors are grateful for the hospitality of Chalk River Labs and TRIUMF during the course of this work. Technical support from Ron Donaberger, Ian Swainson (Chalk River), and Syd Kreitzman (TRIUMF) is greatly appreciated. C.R.W. would like to acknowledge support from NSERC. This work was also supported by grants to J.E.G. and G.M.L. through NSERC, and additional funding to G.M.L. by the CIAR. The MAGLAB experimental apparatus was purchased through funding from the CFI and OIT. Research at Columbia was supported by the U.S. National Science Foundation (DMR-01-02752, CHE-01-17752).

*Corresponding author.
Email address: greedan@mcmaster.ca

[1] *Magnetic Systems with Competing Interactions*, edited by H. T. Diep (World Scientific, New York, 1994).
[2] P. Anderson, Mater. Res. Bull. **8**, 153 (1973).
[3] J. Orenstein and A. J. Millis, Science **288**, 468 (2001).
[4] L. O. Manuel and H. A. Ceccatto, Phys. Rev. B **60**, 9489 (1999).
[5] J. E. Greedan, J. Mater. Chem. **11**, 37 (2001).
[6] C. Lhuillier and G. Misguich, Lecture notes of Cargese summer school in ''Trends in high magnetic field science,'' May 2001.
[7] B. Canals and C. Lacroix, Phys. Rev. Lett. **80**, 2933 (1998).
[8] L. Pauling, *The Nature of the Chemical Bond* (Cornell University Press, Ithaca, 1960).
[9] X. Obradors, A. Labarta, A. Isalgue, J. Tejada, J. Rodriguez, and M. Pernet, Solid State Commun. **65**, 189 (1988).
[10] I. S. Hagemann, Q. Huang, X. P. A. Gao, A. P. Ramirez, and R. J. Cava, Phys. Rev. Lett. **86**, 894 (2001).
[11] J. S. Gardner, B. D. Gaulin, S.-H. Lee, C. Broholm, N. P. Raju, and J. E. Greedan, Phys. Rev. Lett. **83**, 211 (1999).
[12] J. S. Gardner, S. R. Dunsiger, B. D. Gaulin, M. J. P. Gingras, J. E. Greedan, R. F. Kiefl, M. D. Lumsden, W. A. MacFarlane, N. P. Raju, J. E. Sonier, I. Swainson, and Z. Tun, Phys. Rev. Lett. **82**, 1012 (1999).
[13] J. Longo and R. Ward, J. Am. Chem. Soc. **83**, 2816 (1961).
[14] C. G. Shull, E. O. Wollan, and W. A. Strauser, Phys. Rev. **81**, 483 (1950).
[15] H. Kato, T. Okuda, Y. Okimoto, Y. Tomioka, K. Oikawa, T. Kamiyama, and Y. Tokura, Phys. Rev. B **65**, 144404 (2002).
[16] M. Hanawa, Y. Muraoka, T. Tayama, T. Sakakibara, J. Yamaura, and Z. Hiroi, Phys. Rev. Lett. **87**, 187001 (2001).
[17] C. R. Wiebe, J. E. Greedan, G. M. Luke, and J. S. Gardner, Phys. Rev. B **65**, 144413 (2002).
[18] A. Ferretti, D. B. Rogers, and J. B. Goodenough, J. Phys. Chem. Solids **26**, 2007 (1965).
[19] DICVOL Version 24/11/98.
[20] FULLPROF Version 3.5d (Oct. 98).
[21] R. D. Shannon, Acta Crystallogr., Sect. A: Cryst. Phys., Diffr., Theor. Gen. Crystallogr. **32**, 751 (1976).
[22] V. V. Gagulin, Segnetoelektriki P'ezoelektriki **4**, 128 (1987).
[23] D. Iwanaga, Y. Inaguma, and M. Itoh, Mater. Res. Bull. **35**, 449 (2000).
[24] *Muons in Physics, Chemistry, and Materials, Proceedings of the Fifty First Scottish Universities Summer School in Physics*, edited by S. L. Lee and R. Cywinski (Institute of Physics, University of Reading, Berkshire, 1999).
[25] A. P. Ramirez, in *Handbook of Magnetic Materials*, edited by K. H. J. Buschow (North-Holland, Amsterdam, 2001), Vol. 13, p. 423.
[26] Y. J. Uemura, T. Yamazaki, D. R. Harshman, M. Senba, and E. J. Ansaldo, Phys. Rev. B **31**, 546 (1985).
[27] J. A. Mydosh, *Spin Glasses, An Experimental Introduction* (Taylor and Francis, London, 1993).
[28] S. R. Dunsiger, R. F. Kiefl, K. H. Chow, B. D. Gaulin, M. J. P. Gingras, J. E. Greedan, A. Keren, K. Kojima, G. M. Luke, W. A. MacFarlane, N. P. Raju, J. E. Sonier, Y. J. Uemura, and W. D. Wu, Phys. Rev. B **54**, 9019 (1996).
[29] L. Limot, P. Mendels, G. Collin, C. Mondelli, B. Ouladdiaf, H. Mutka, N. Blanchard, and M. Mekata, Phys. Rev. B **65**, 144447 (2002).
[30] M. Bieringer, N. P. Raju, G. M. Luke, and J. E. Greedan, Phys. Rev. B **62**, 6521 (2000).
[31] A. P. Ramirez, B. Hessen, and M. Winkelmann, Phys. Rev. Lett. **84**, 2957 (2000).
[32] P. Sindzingre, C. Misguich, C. Lhuillier, B. Bernu, L. Pierre, Ch. Waldtmann, and H.-U. Everts, Phys. Rev. Lett. **84**, 2953 (2000).
[33] A. S. Wills, A. Harrison, S. A. M. Mentink, T. E. Mason, and Z. Tun, Europhys. Lett. **42**, 325 (1998).
[34] W. E. Fogle, J. D. Boyer, R. A. Fisher, and N. E. Philips, Phys. Rev. Lett. **50**, 1815 (1983).